Available online at www.sciencedirect.com
SCIENCE DIRECT®
Journal of Catalysis 224 (2004) 1–7
JOURNAL OF CATALYSIS
www.elsevier.com/locate/jcat

Propane oxidative dehydrogenation on VO_x/ZrO_2 catalysts

C.L. Pieck,*,[1] M.A. Bañares, and J.L.G. Fierro

Instituto de Catálisis y Petroleoquímica, CSIC, Campus Cantoblanco, E-28049 Madrid, Spain

Received 4 August 2003; revised 4 November 2003; accepted 16 February 2004

Abstract

The catalytic properties of the V_2O_5/ZrO_2 system for the oxidative dehydrogenation of propane were studied. Catalysts with different chemical compositions (i.e., vanadium oxide loadings) were prepared, with activation done by calcination at two temperature levels. Samples were characterized by nitrogen adsorption, temperature-programmed reduction, and Raman and photoelectron spectroscopic techniques. It was found that calcination temperature level strongly affects the structure of ZrO_2 (tetragonal zirconia predominates at 500 °C while the transformation to a monoclinic phase occurs at 650 °C). The calcination temperature also affects the nature of vanadium oxide species on the surface of ZrO_2. After calcination at 500 °C surface vanadium oxide species are formed at low vanadium loadings, but crystalline V_2O_5 structures appear at the higher ones. Calcination at 650 °C leads to the formation of ZrV_2O_7, mainly at high vanadium loadings. The results of propane oxidative dehydrogenation show that surface-isolated vanadium oxide species are more selective to C_3H_6. On the other hand, it was found that the catalysts suffer a slow deactivation during reaction due to ZrV_2O_7 formation. This transformation decreases the activity but the activity-selectivity profile is not affected.

Keywords: Oxidative dehydrogenation; Propane; Vanadium-supported catalysts

1. Introduction

The widespread use of alkenes as raw materials for the petrochemical industry makes their intrinsic value considerably higher than those of the corresponding alkanes from which they can be produced by dehydrogenation at high temperatures (> 600 °C). High-temperature processes have several disadvantages including formation of undesirable cracking products, and high catalyst deactivation rates by coking leading to frequent catalyst regeneration, and it is energy intensive due to the endothermic nature of dehydrogenation. For this reason, the use of oxidative dehydrogenation as an alternative route to produce olefins is receiving increasing attention nowadays. The presence of oxygen would produce a net exothermicity due to the coupling of strongly exothermic hydrogen oxidation, bringing additionally the benefits of reduced coke formation. The main drawbacks of this catalytic approach to convert alkanes to alkenes are that the activation of alkane molecules is difficult and frequently unspecific so alkene yields are poor due to the formation of undesirable oxidation by-products (CO_x), which are thermodynamically more stable.

Several catalyst types have been studied for oxidative dehydrogenation of propane; among them, supported vanadium has received considerable attention [1–8]. Many hypotheses have been proposed about the nature of the active sites involved in alkane oxidative dehydrogenation. Regarding the oxidation state of vanadium oxide, some authors [9–11] proposed that tetrahedral V^V species are active for dehydrogenation, but other authors [12–14] link their activity to the V^V/V^{IV} redox pair. In situ UV–vis and Raman reaction studies of supported vanadium oxide catalysts for the selective oxidation of light paraffins (ethane, propane, butane) show that during such redox cycles, surface vanadium oxide species are essentially present as V^V, with a very moderate extent of reduction [15–17]. Changes in the oxidation states of vanadium oxide species during propane oxidative dehydrogenation reaction were also reported [7,8,18]. These changes were explained using a Mars–Van Krevelen redox mechanism involving lattice oxygen atoms [1,5]. It has been also reported that the higher selectivity exhibited by Mg pyrovanadate is due to its ability to stabilize V^{IV} associated with oxygen vacancies [19]. It is well known that tetrahe-

* Corresponding author. INCAPE, Santiago del Estero 2654, 3000 Santa Fe, Argentina. Fax: 54 342 4531068.
E-mail address: pieck@fiqus.unl.edu.ar (C.L. Pieck).
[1] On leave from INCAPE and guest researcher at CSIC.

0021-9517/$ – see front matter
doi:10.1016/j.jcat.2004.02.024

dral vanadium species are the active ones but there exists some controversy about the influence of its chemical environment. Some authors have linked olefin selectivity to the presence of isolated VO_4 tetrahedra [20,21], but evidence has also been found about the pyrovanadate species (V_2O_7) as the important ones [12,22]. Khodakov et al. [2] suggest that monovanadates structures are significantly less active than polyvanadates. It has been also demonstrated that active centers are V–O–support regarding the strong influence of the support on both activity and selectivity [15,23–26]. While V=O species have been found responsible for deep oxidation leading to CO_x [27], this functionality is not critical for the selective oxidation of paraffins to olefins on supported oxides [15,16,24–26,28–31].

In this paper we report on the roles of vanadium oxide loading and activation temperature in the zirconia-supported VO_x system as catalyst for the oxidative dehydrogenation of propane.

2. Experimental

As support, $Zr(OH)_4$ stabilized with 3.5% SiO_2 (MEL Chemical) was calcined at 650 °C under air atmosphere to obtain ZrO_2.

V/ZrO_2 catalysts were prepared in a rotatory evaporator (Büchi 461). The support (ZrO_2), aqueous HNO_3 (pH 2), and the required amount of NH_4VO_3 were processed at 80 °C under vacuum (0.7 atm) until dryness. The obtained powder was then further dried in an oven at 120 °C overnight. Samples were finally calcined under air at 500 or 650 °C for 4 h. Catalysts were prepared to obtain 0.2, 0.5, 1, and 2 vanadium monolayers and were denominated 0.2 V/ZrO_2, 0.5 V/ZrO_2, etc. A suffix indicates the calcination temperature of the catalyst (−500 or −650 °C). The monolayer content was calculated by considering the surface density of vanadium oxide coverage of 9 vanadium atoms per square nanometer of the original surface area of ZrO_2.

ZrV_2O_7 was prepared by mixing of aqueous NH_4VO_3 and the required amount of $Zr(OH)_4$ for a V/Zr atomic ratio of 2. Excess water was eliminated using a rotatory evaporator under the same conditions previously noted. Powder samples were dried at 120 °C overnight and then calcined 24 h at 700 °C.

For temperature-programmed reduction, a Micromeritics TPR/TPD 2000 equipment with a thermal-conductivity detector was used. The reducing media was H_2 (5%) in Ar at 50 cm^3/min. Temperature was linearly raised at 10 °C/min. Samples were previously heated at 150 °C under He for 1 h to eliminate residual moisture.

BET area was determined by N_2 adsorption at −196 °C (BET method). Adsorption isotherms were obtained using Micromeritics ASAP 2000 equipment. Samples were previously degassed at 140 °C for 2 h.

Raman spectra were obtained in a equipment capable of operation at different temperatures under controlled atmosphere with a Renishaw System 1000 apparatus equipped with a single monochromator, a CCD detector cooled at −73 °C, and a holographic super-Notch filter. The filter rejects the elastic scattering so that the Raman signal remains higher than when triple monochromator spectrometers are used. The samples were excited with a 514 nm Ar laser. Spectral resolution was ca. 3 cm^{-1} and spectrum acquisition consisted of ten 30-s accumulations. The spectra were obtained under dehydrated conditions (120 °C) in a hot stage plate (Linkam TS-1500) in a flow of dry air. Hydrated samples were obtained at room temperature during exposure to a stream of humid synthetic air.

X-ray photoelectron spectra were recorded with a VG Escalab 200R electron spectrometer equipped with a hemispherical electron analyzer, using an Mg-K_α ($h\nu = 1253.6$ eV) X-ray source. The energy regions of V 2p–O 1s, Zr 3d, and C 1s levels were scanned at a pass energy of 20 eV and signal-averaged for 90 scans. These conditions are appropriate for obtaining good signal-to-noise ratios. A PDP 11/04 computer (Digital) was used to record and analyze the spectra. Calculating the integral of each peak after subtraction of an S-shaped background and fitting the experimental curve to a combination of Gaussian and Lorentzian lines estimated peak intensities. The C1s peak (contamination) at a binding energy (BE) of 284.9 eV was taken as an internal standard for BE measurements.

Propane oxidative dehydrogenation runs were done using a quartz reactor with 50 mg catalyst samples. Reacting mixture was propane/oxygen/helium molar ratio of 1/2/4 at atmospheric pressure. Flow was kept at 30 cm^3/min and reaction temperature was varied in the range 340–640 °C. Products were analyzed using a gas chromatograph with TCD.

Experimental data of propane conversion at different temperature levels were used in order to obtain the activation energy assuming first-order reaction and a plug-flow reactor model (unidimensional):

$$W/F_A = \int \frac{dX}{r_A}. \tag{1}$$

Catalytic reaction was supposed to proceed under net kinetic control; i.e., that no diffusional effects restricted the mass transfer inside the catalyst pores or the gas film surrounding the catalyst pellets. This hypothesis was checked by evaluating the Weisz–Prater criterion and Damköhler number for the maximum values of observed reaction rates.

3. Results and discussion

In some previous works [32,33] we have reported results on characterization of V/ZrO_2 catalysts calcined at 650 °C using BET, XRD, and Raman techniques. It was found that ZrO_2 had a tetragonal structure after calcining at 650 °C. It was also found that the presence of dispersed vanadium oxide species on ZrO_2 affects the structure of zirconia and the

BET area after calcination. As vanadium coverage increases, the transition from the tetragonal to monoclinic polymorph is more extensive. At high vanadium coverage, the BET area decreases remarkably. Vanadium coverage also promotes the formation of ZrV_2O_7, which appears to originate from the intimate contact between dispersed vanadium oxide species and the zirconia support. It was also reported that surface vanadium oxide species are formed at low vanadium content and V_2O_5 forms at high vanadium oxide loading. ZrV_2O_7 forms more easily from surface vanadium oxide species than from crystalline V_2O_5 [32].

Fig. 1 shows the influence of vanadium monolayer coverage on the specific surface area of the catalysts after calcination at 500 and 650 °C. The support alone, calcined at 650 °C, has a surface area of 86 m^2/g. The reference ZrV_2O_7 has a very low surface area (< 1 m^2/g). BET area values decrease with vanadium oxide loading for both series. Catalysts calcined at 650 °C possess surface area values substantially lower at any vanadium loading level than the ones calcined at 500 °C. For the former catalysts a sharp decrease in surface area with V loading up to monolayer coverage can be observed, this decreasing being less steep at higher vanadium contents. In the case of catalysts calcined at 500 °C a linear, less intense decrease of surface area with vanadium loading was observed. The linear decrease in the BET area of samples calcined at 500 °C is attributed to a progressive blocking over the narrows pores of the support by the surface vanadium oxide species. A previous XRD study excludes the development of large ZrO_2 crystals as a cause for the decrease in the area of this series; however, the decrease of the BET area of the samples calcined at 650 °C is basically related to the crystallization of the support substrate [32]. Both the presence of vanadium oxide species on ZrO_2 and the zirconia crystal growth at high temperature affect the BET area values.

Raman spectra for catalysts calcined at 500 °C are shown in Fig. 2. It can be seen that the presence of 0.2 vanadium monolayers induces a phase change to monoclinic (Raman bands at 187, 383, and 477 cm^{-1} [34]). A hydration-sensitive Raman band at 1010 cm^{-1} of the V=O stretching mode of surface vanadium oxide species is observed. The increasing presence of vanadium oxide strongly diminishes the intensity of the ZrO_2 Raman bands. 0.5 V/ZrO_2-500 °C exhibits no Raman bands of ZrO_2, but possesses a broad Raman band near 900–1010 cm^{-1} along with broad Raman features near 280, 300, 410, 530, and 700 cm^{-1}, which sharpen with vanadia monolayer coverage. The new Raman bands are those of crystalline V_2O_5 (990, 701, 528, 407, 303, 283, and 141 cm^{-1}). 1 V/ZrO_2-500 °C still exhibits the Raman band at 1010 cm^{-1}, so some surface vanadium oxide species coexist; but this species is no longer observed in 2 V/ZrO_2-500 °C.

The BE values of the V $2p_{3/2}$ peak and the relative XPS V/Zr atomic ratios are summarized in Table 1 for the catalysts calcined at 650 and 500 °C. The V $2p_{3/2}$ core-level spectra for V/ZrO_2 catalysts were satisfactorily fitted to two components: the peaks at higher BE of 517.6–517.7 eV and at lower BE (516.6–516.8 eV) are assigned to V^V and V^{IV} species, respectively [35]. The relative abundance of V^{IV}/V_{total} was also calculated from the fitting of the experi-

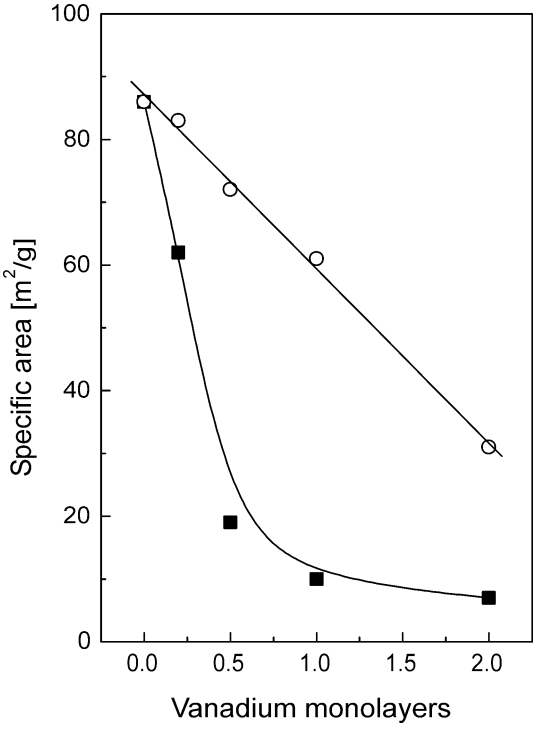

Fig. 1. BET specific area as a function of the number of vanadium monolayers. Catalysts calcined at 650 °C (■) and 500 °C (◯).

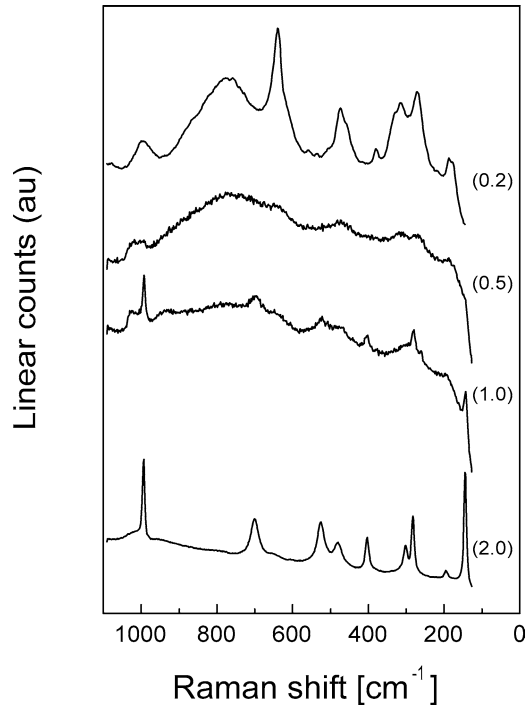

Fig. 2. Raman spectra of dehydrated V/ZrO_2 calcined at 500 °C. Numbers in parentheses indicate the number of vanadium monolayers.

Table 1
Surface atomic ratios as obtained by XPS

		650 °C		500 °C	
Monolayers	V/Zr bulk	V/Zr surface	V^{IV}/V_{total}	V/Zr surface	V^{IV}/V_{total}
0.2	0.033	0.127	0.36	0.082	0.33
0.5	0.082	0.250	0.32	0.209	0.33
1.0	0.135	0.257	0.23	0.279	0.22
2.0	0.270	0.355	0.22	0.512	0.00

mental peaks. These values are also summarized in Table 1. For the catalysts calcined at 650 °C, the proportion of V^{IV} ions decreases upon increasing the vanadium content in the catalysts (from 0.36 in 0.2 V/ZrO_2 to 0.22 in 2.0 V/ZrO_2). This points to the stabilization of a relatively higher proportion of V^{IV} in samples at lower vanadium contents with respect to that at higher vanadium loading. The same phenomenon occurs for catalysts calcined at 500 °C. It is important to point out that 2 V/ZrO_2 exhibits a single component at 517.5 eV, characteristic of V^{V} species.

Surface atomic ratios were calculated from the XPS peak intensity ratios, normalized by atomic sensitivity factors [30]. For the catalysts calcined at 650 °C, the surface V/Zr atomic ratio sharply increases when passing from 0.2 to 0.5 monolayers. At higher coverage, it increases at a lower rate, which indicates that there must be an aggregation of vanadium oxide species. For the catalysts calcined at 500 °C, it can be seen that the V/Zr surface atomic ratio continuously increases with vanadium oxide loading. This trend suggests that the dispersion of vanadium oxide on zirconia support is higher for the series calcined at 500 °C.

Fig. 3 shows the TPR profiles of the V/ZrO_2 catalysts calcined at 500 and 650 °C and ZrV_2O_7 as reference compound. Supported vanadium oxide is reduced at lower temperatures than bulk V_2O_5. Only one peak near 400 °C is detected at low vanadium contents (0.2 and 0.5 monolayers of vanadium), regardless of the calcination temperature. This peak is not shifted to higher temperatures and can therefore correspond to the reduction of surface vanadium oxide species. Catalysts calcined at 500 °C have only one reduction peak which shifts to higher temperatures with vanadium loading. The TPR profile of bulk V_2O_5 exhibits reduction peaks at 655, 686, and 807 °C [27,33,36,37]. Therefore, the shift to higher temperature values may be indicative of an incipient formation of the V_2O_5 phase. Particularly noticeable is the shift observed when vanadium loading increases from 1 to 2 monolayers (ca. 95 °C) in the V/ZrO_2-500 °C series. Therefore, it may be concluded that catalyst 2 V/ZrO_2 must have V_2O_5 crystals in higher proportion than the catalysts with a lower vanadium content, which is consistent with the Raman spectra. The series calcined at 650 °C presents rather different profiles at monolayer coverage and above. The Raman spectra indicate that the 1 V/ZrO_2-650 °C possesses V_2O_5 and ZrV_2O_7. This series exhibits the ZrV_2O_7 phase at two monolayers of vanadia. ZrV_2O_7 exhibits the reduction peaks (428, 546, and 581 °C) [32,33]. The reduction peaks appearing of $2V/ZrO_2$-650 °C are reasonably consistent with the presence of ZrV_2O_7, which displays three reduction peaks at lower temperatures than those of V_2O_5. For the 1 V/ZrO_2-650 °C catalyst, the reduction peak near 500 °C must be assigned to the V_2O_5, and may also have a component from the first reduction peak of ZrV_2O_7. The other two reduction peaks at higher temperature values may be indicative of the reduction of ZrV_2O_7.

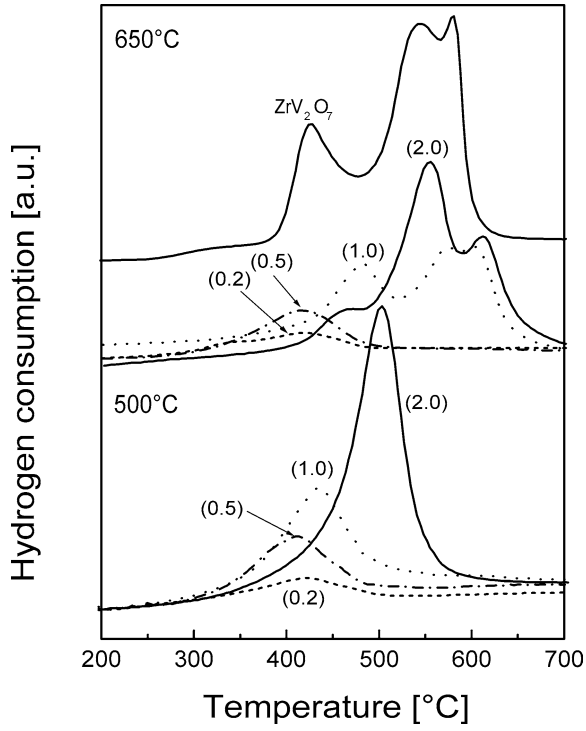

Fig. 3. Temperature-programmed reduction plots of V/ZrO_2 catalyst calcined at 650 and 500 °C and ZrV_2O_7. Numbers in parentheses indicate the number of vanadium monolayers.

The values of propane conversion as a function of reaction temperature are shown in Fig. 4. It can be seen that all catalysts have better activity than the support. ZrV_2O_7 as prepared in this work as reference exhibited very low activity (1.5% conversion at 640 °C). For catalysts calcined at 500 °C, activity increases with vanadium loading up to 1 vanadium monolayer loading but then decreases at higher vanadium loading (2 V/ZrO_2-500 °C catalyst). The initial increase in activity with vanadium content may be associated with the increase in concentration of surface vanadium oxide species. The lower activity of 2 V/ZrO_2-500 °C must be ascribed to the presence of considerable amounts of crystalline

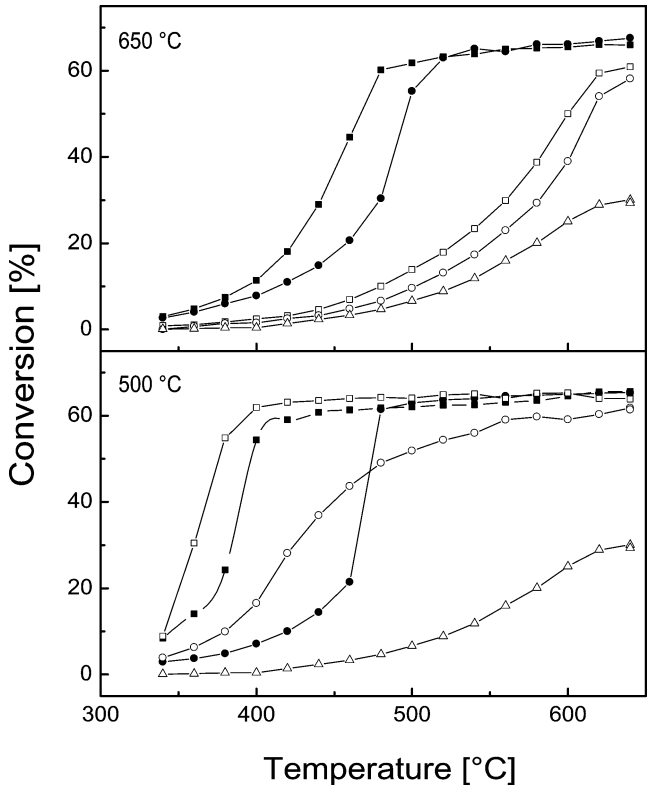

Fig. 4. Conversion of propane as a function of the temperature of reaction: (●) 0.2 V monolayers, (■) 0.5 V monolayers, (□) 1.0 V monolayers, (○) 2.0 V monolayers. Triangle is ZrO_2.

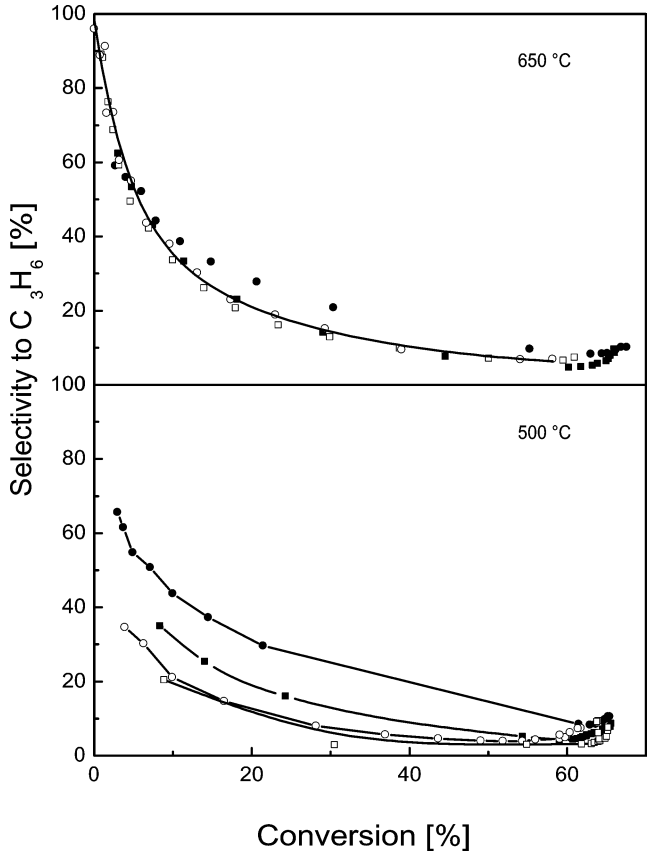

Fig. 5. Selectivity to C_3H_6 as a function of the degree of conversion of C_3H_8 for catalysts calcined at 650 and 500 °C. Symbols as in Fig. 4.

V_2O_5 that decrease the number of surface sites. The catalyst 1 V/ZrO_2-500 °C is the most active in the series despite the presence of V_2O_5 crystals. The total amount of these crystals is low but their very high Raman section, ca. 30 times that of surface vanadia species [38], affords a Raman spectrum dominated by a V_2O_5 crystalline phase. However, the total amount of crystalline vanadia is significantly lower than it appears. This is consistent with the TPR profiles, which show a reduction temperature significantly lower than catalyst 2 V/ZrO_2-500 °C, which predominantly possesses V_2O_5 crystals. Thus, its reduction profile is dominated by that of the surface vanadium oxide species.

For catalysts calcined at 650 °C, a similar behavior was noted, with an increase in activity with vanadium content for the lower vanadium loadings (0.2 and 0.5 V/ZrO_2 catalysts) and a considerable decrease in activity for the higher vanadium loadings. In this case the loss of activity may be associated with ZrV_2O_7 formation due to the higher calcination temperature level (ZrV_2O_7 has very low catalytic activity). The strong decrease in surface area with vanadium loading for this catalysts series must be taken into account as a possible concurrent cause of activity loss.

In Fig. 5, the values of propane selectivity as a function of propane conversion are presented. Catalysts calcined at 650 °C have virtually the same selectivity level despite its vanadium content, being the 0.2 V/ZrO_2-650 °C slightly more selective. The better selectivity profile of the 650 °C despite its low activity may be due to the low reactivity of surface sites upon formation of zirconium vanadate, which possesses a very low activity. For the 500 °C series, a decrease on selectivity as vanadium loading increases was noted. This behavior must be attributed to the decrease of surface vanadium oxide species population due to the presence of a crystalline vanadia phase. The catalysts calcined at 650 °C have the same selectivity-conversion curve regardless of the V^{IV}/V_{total} ratio. It changes from 0.36 to 0.22. The catalyst with the highest selectivity to C_3H_6 is 0.2 V/ZrO_2-500 °C. This catalyst has the highest amount of surface vanadium oxide species. This could be in line with the role of isolated surface vanadium oxide species as the active sites, as reported by Corma et al. [20] and Michalakos et al. [21].

In order to study the stability of these catalysts a second reaction test was performed using the 0.5 V/ZrO_2-650 °C catalyst. A plot of conversion values as a function of temperature corresponding to these two successive tests can be found in Fig. 6. After the first reaction cycle, a drop in catalytic activity is found. However, the conversion versus C_3H_6 selectivity profile remains the same, suggesting that while the amount of active sites decreases, the relative concentration of different active sites remains the same. This is consistent with the constancy of the activation energy for this catalyst before and after deactivation as seen in Fig. 7 where the classical Arrhenius plots are presented.

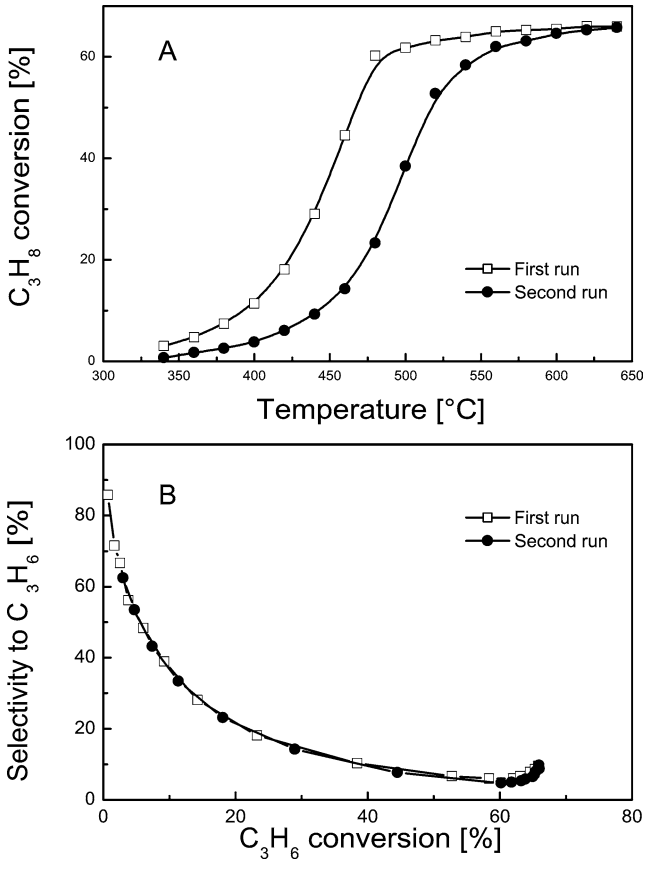

Fig. 6. (A) Conversion of propane as a function of the temperature of reaction of 0.5 V/ZrO_2-650 °C in successive runs. (B) Selectivity to C_3H_6 as a function of the degree of conversion of C_3H_8 in successive runs.

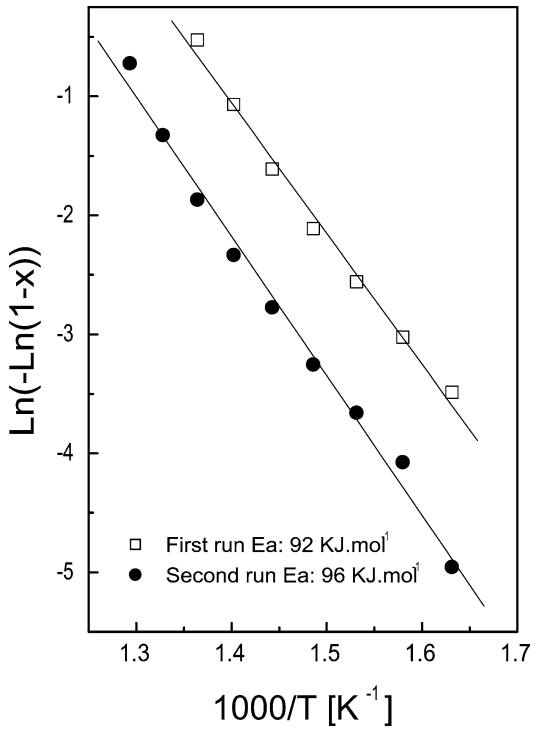

Fig. 7. Activation energy of 0.5 V/ZrO_2-650 °C catalyst in first and second test reactions.

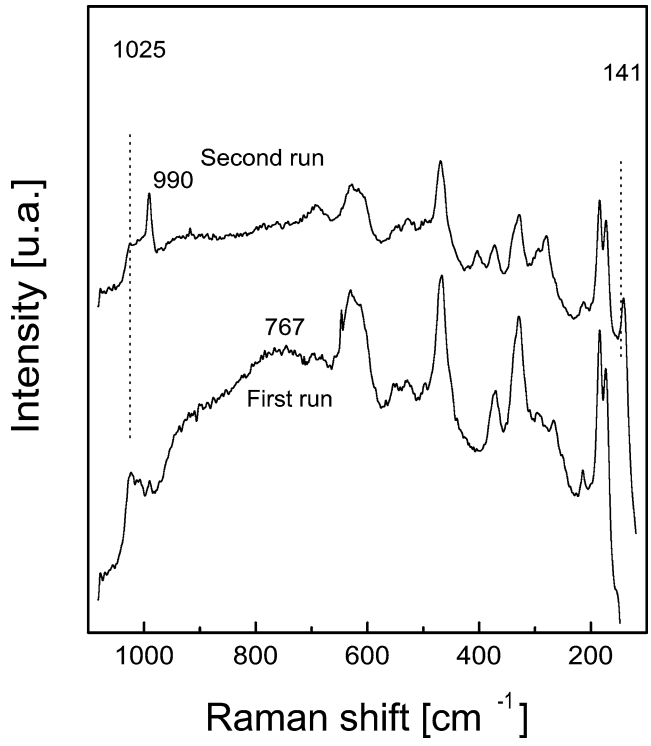

Fig. 8. Raman spectra of fresh and used 0.5 V/ZrO_2-650 °C catalyst.

Fig. 8 shows the Raman spectra of the catalyst 0.5 V/Zr-650 °C after the first and second catalytic run. The Raman spectra show a moderate rearrangement of surface vanadium oxide species toward the formation of crystalline V_2O_5 and ZrV_2O_7. The formation of ZrV_2O_7 must be very incipient as the broadness of the Raman feature at 767 cm^{-1} suggests. The size of the V_2O_5 crystallites must be very small since the Raman section of V_2O_5 crystals is ca. 30 times higher than that of surface vanadium oxide species [38]. The most intense Raman bands of crystalline V_2O_5 at 147 and 994 cm^{-1} are moderately more intense than those of surface vanadia. Thus, most vanadia remains exposed, and only a minimal fraction has aggregated as V_2O_5 in line with the data of Iglesia and co-workers [38]. It does appear that some surface vanadium oxide also interacts with zirconia support forming ZrV_2O_7. V_2O_5 is active for propane ODH, but the fraction of exposed vanadia sites decreases. However, the total amount of V_2O_5 appears too little to have an appreciable effect. ZrV_2O_7 is not active for propane ODH; therefore, it appears that the incipient formation of ZrV_2O_7 must account for the deactivation of V/ZrO_2 catalysts. The constancy in the activation energy values and the identity of conversion-selectivity profiles suggest that the decrease in activity may be due to a decrease in the number of active sites rather than to a change in the nature of the active site. This may be indicative of the relevance of the V–O–Zr bond, which is present in both zirconia-supported vanadium oxide and ZrV_2O_7 phase.

4. Conclusions

The calcination temperature influences the nature of surface vanadium oxide species over zirconia. At 500 °C, dispersed surface species are formed when low vanadium loadings are used and V_2O_5 bulk crystalline species are formed at high loading. At 650 °C only a small percentage of surface species is produced, and most vanadium is present in the form of oxide crystals. V_2O_5 is the main form while at high vanadium loading ZrV_2O_7 is also present.

All the different vanadium oxide species present on the catalyst have some influence over the catalytic activity, but isolated VO_4 species have the highest activity and selectivity to C_3H_6. The V^{IV}/V_{total} ratio has seemingly little influence over the conversion level or the selectivity. The Raman spectra of used catalyst show little formation of ZrV_2O_7 during the test reaction. These changes induce an activity decrease but the selectivity-conversion profile and the activation energy values remain constant. This behavior suggests that the nature of the active sites of fresh and used catalyst must be the same. Therefore, only the number of active sites would be changing. It makes sense to assume that the V–O–Zr bond must be directly involved in the rate-determining step for propane ODH on V–Zr–O systems.

Acknowledgments

C.L.P. thanks the Spanish Ministry of Education for a grant to fund his stay in Spain. This research was partly funded by the EU under Project BE-1169 and by CICYT Project QUI98-0784.

References

[1] K. Chen, A. Khodakov, J. Yang, A.T. Bell, E. Iglesia, J. Catal. 186 (1999) 325.
[2] A. Khodakov, B. Olthof, A.T. Bell, E. Iglesia, J. Catal. 181 (1999) 205.
[3] A. Khodakov, J. Yang, S. Su, E. Iglesia, A.T. Bell, J. Catal. 177 (1998) 343.
[4] E.A. Mamedov, V. Cortés Corberán, Appl. Catal. A 127 (1995) 1.
[5] K. Chen, A.T. Bell, E. Iglesia, J. Catal. 209 (2002) 35.
[6] B. Grzybowska, J. Sloczynki, R. Grabowski, K. Samson, I. Gressel, K. Wcislo, L. Gengembre, Y. Barbaux, Appl. Catal. A 230 (2002) 1.
[7] X. Gao, J. Jehng, I.E. Wachs, J. Catal. 209 (2002) 43.
[8] G. García Cortez, M.A. Bañares, J. Catal. 209 (2002) 197.
[9] B. Solsona, T. Blasco, J.M. López Nieto, J.M.L. Peña, F. Rey, A. Vidal-Moya, J. Catal. 203 (2001) 443.
[10] R. Monaci, E. Rombi, V. Solinas, A. Sorrentino, E. Santacesaria, G. Colon, Appl. Catal. A 214 (2001) 203.
[11] T. Blasco, J.M. López Nieto, Appl. Catal. A 157 (1997) 117.
[12] D. Siew Hew Sam, V. Soenen, J.C. Volta, J. Catal. 123 (1990) 417.
[13] M.A. Chaar, D. Patel, M.C. Kung, H.H. Kung, J. Catal. 105 (1987) 483.
[14] G. Garcia Cortez, J.L.G. Fierro, M.A. Bañares, Catal. Today 78 (2003) 219.
[15] M.A. Bañares, M.V. Martínez-Huerta, X. Gao, J.L.G. Fierro, I.E. Wachs, Catal. Today 61 (2000) 295.
[16] I.E. Wachs, J.-M. Jehng, G. Deo, B.M. Weckhuysen, V. Guliants, J.B. Benziger, Catal. Today 32 (1996) 47.
[17] G. Deo, K. Seshan, I.E. Wachs, J.A. Lercher, Catal. Today 28 (1996) 139.
[18] B.P. Barbero, L.E. Cadús, H. Hilaire, Appl. Catal. A 246 (2003) 237.
[19] A. Guerrero Ruiz, I. Rodriguez Ramos, J.L.G. Fierro, V. Soenen, J.M. Herrman, J.C. Volta, Stud. Surf. Sci. Catal. 72 (1992) 203.
[20] A. Corma, J.M. López Nieto, N. Paredes, J. Catal. 144 (1993) 425.
[21] P.M. Michalakos, M.C. Kung, L. Jahan, H.H. Kung, J. Catal. 140 (1993) 226.
[22] T. Lindblad, B. Rebenstorf, Z.G. Yan, S.L.T. Andersson, Appl. Catal. A 112 (1994) 187.
[23] R.H.H. Smits, K. Seshan, H. Leemresize, J.R.H. Ross, Catal. Today 16 (1993) 513.
[24] M.A. Bañares, X. Gao, J.L.G. Fierro, I.E. Wachs, Stud. Surf. Sci. Catal. 110 (1997) 295.
[25] M.A. Bañares, I.E. Wachs, J. Raman, Spectroscopy 33 (2002) 359.
[26] I.E. Wachs, J.-M. Jehng, G. Deo, B.M. Weckhuysen, V.V. Guliants, J.B. Benziger, S. Sundaresan, J. Catal. 170 (1997) 75.
[27] H. Bosch, B.J. Kip, J.G. van Ommen, P.J. Gellings, J. Chem. Soc., Faraday Trans. 180 (1984) 2479.
[28] N.K. Nag, K.V.R. Chary, B.R. Rao, V.S. Subrahmanyam, Appl. Catal. 31 (1987) 73.
[29] M. Faraldos, M.A. Bañares, J.A. Anderson, H. Hu, I.E. Wachs, J.L.G. Fierro, J. Catal. 160 (1996) 214.
[30] C.D. Wagner, L.E. Davis, M.V. Zeller, J.A. Taylor, R.H. Raymond, L.H. Gale, Surf. Interface Anal. 3 (1981) 211.
[31] M.A. Bañares, M. Martínez-Huerta, X. Gao, I.E. Wachs, J.L.G. Fierro, Stud. Surf. Sci. Catal. A 130 (2000) 3125.
[32] C.L. Pieck, M.A. Bañares, M.A. Vicente, J.L.G. Fierro, Chem. Mater. 13 (2001) 1174.
[33] C.L. Pieck, S. Del Val, M. López Granados, M.A. Bañares, J.L.G. Fierro, Langmuir 18 (2002) 2642.
[34] J.R. Sohn, S.G. Cho, Y.L. Pae, S. Hayashi, J. Catal. 159 (1996) 170.
[35] D. Briggs, M.P. Seah (Eds.), Practical Surface Analysis. Auger and X-Ray Photoelectron Spectroscopy, Wiley, Chichester, 1990.
[36] G.C. Bond, J. Perez Zurita, S. Flamerz, P.J. Gellings, H. Bosh, J.G. Van Ommen, B.J. Kip, Appl Catal. 22 (1986) 361.
[37] M.-M. Koranne, J.G. Goodwin Jr., G. Marcellin, J. Catal. 148 (1994) 369.
[38] S. Xie, E. Iglesia, A.T. Bell, J. Phys. Chem. B 105 (2001) 5144.